EURASIP Journal on Wireless Communications and Networking 2005:4, 493–504

MAC Protocols for Optimal Information Retrieval Pattern in Sensor Networks with Mobile Access

Zhiyu Yang
School of Electrical and Computer Engineering, Cornell University, Ithaca, NY 14853, USA
Email: zy26@cornell.edu

Min Dong
Corporate Research & Development, QUALCOMM Incorporated, 5775 Morehouse Drive, San Diego, CA 92121, USA
Email: mdong@qualcomm.com

Lang Tong
School of Electrical and Computer Engineering, Cornell University, Ithaca, NY 14853, USA
Email: ltong@ece.cornell.edu

Brian M. Sadler
Army Research Laboratory, Adelphi, MD 20783-1197, USA
Email: bsadler@arl.army.mil

Received 9 December 2004

In signal field reconstruction applications of sensor network, the locations where the measurements are retrieved from affect the reconstruction performance. In this paper, we consider the design of medium access control (MAC) protocols in sensor networks with mobile access for the desirable information retrieval pattern to minimize the reconstruction distortion. Taking both performance and implementation complexity into consideration, besides the optimal centralized scheduler, we propose three decentralized MAC protocols, namely, decentralized scheduling through carrier sensing, Aloha scheduling, and adaptive Aloha scheduling. Design parameters for the proposed protocols are optimized. Finally, performance comparison among these protocols is provided via simulations.

Keywords and phrases: medium access control, signal field reconstruction, sensor networks.

1. INTRODUCTION

In many applications, sensor networks operate in three phases: sensing, information retrieval, and information processing. As a typical example, in physical environmental monitoring, sensors first take measurements of the signal field at a particular time. The data are then collected from individual sensors to a central processing unit, where the signal field is finally reconstructed.

An appropriate network architecture for such applications is SEnsor Networks with Mobile Access (SENMA) [1, 2]. As shown in Figure 1, SENMA consists of two types of nodes: low-power low-complexity sensors randomly deployed in a large quantity, and a few powerful mobile access points communicating with the sensors. The use of mobile access points enables data collection from specific areas of the network.

We focus on the latter two operational phases in the SENMA architecture: information retrieval and processing, which are strongly coupled. To achieve the optimal performance of the sensor network, the two phases should be considered jointly. The key to information retrieval is medium access control (MAC) that regulates data retrieval from sensors to the access point. The main focus of this paper is to design MAC protocols for the optimal reconstruction of the signal field.

The MAC design for sensor network applications needs to take into account application-specific characteristics, for example, the correlation of the field, the randomness of the sensor locations, and the redundancy of the large-scale sensor deployment. The traditional MAC design criteria, such as throughput, fail to capture the characteristics of the specific

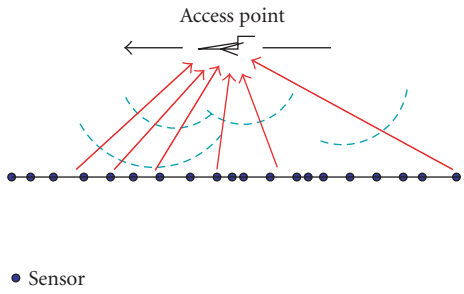

Figure 1: A 1D sensor network with a mobile access point.

sensor application; a high-throughput MAC does not imply low reconstruction distortion. In this paper, we propose a new MAC design criterion for the field reconstruction application.

The new MAC design criterion is motivated by the need to collect data evenly across the field for a given throughput. If we have an infinitely dense network, the optimal data collection strategy is to retrieve samples from evenly spaced locations. For a finite density network considered in this work, however, there may not exist sensors in the desired locations. The optimal centralized scheduler, with the location information of all sensors, calculates the optimal location set and retrieves data from the optimal set to minimize the reconstruction distortion. Such optimal centralized scheduler comes with the substantial cost of sensor-location information gathering. Decentralized MAC protocols, on the other hand, require much less intervention from the mobile access point and bandwidth resources.

We consider a one-dimensional problem for simplicity, which can be extended to a two-dimensional setup. Taking both performance and implementation complexity into consideration, besides the optimal centralized scheduler, we propose three decentralized MAC protocols. We first propose a decentralized scheduler via carrier sensing, which, under the no-processing delay assumption, provides little performance loss compared to the performance of the optimal scheduler. Then, to simplify the implementation, we introduce a MAC scheme which uses Aloha-like random access within a resolution interval centered at the desired retrieval location. Finally, to improve the performance, we propose an adaptive Aloha scheduling scheme which adaptively chooses the desired retrieval locations based on the history of retrieved samples. Design parameters are optimized for the proposed schemes. The performance comparison under various sensor density conditions and packet collection sizes is also provided.

The problems on sensor network communications have attracted a growing research interest. In terms of medium access control, many MAC protocols have been proposed aiming at the special needs and requirements for both ad-hoc sensor networks [3, 4, 5, 6] and sensor networks with mobile access [2]. Most of these proposed schemes only consider the MAC layer performance, that is, throughput. The effect of MAC for information retrieval on information processing is analyzed in [7, 8] for infinite and finite sensor density networks, respectively, where the performance of the centralized scheduler and that of the decentralized random access are analyzed and compared.

The idea of using carrier sensing for energy-efficient transmission in sensor networks was first proposed in [9, 10, 11], where backoff delays are chosen as a function of the channel strength. The carrier sensing strategy presented here generalized that in [9, 10, 11] by using carrier sensing to distinguish nodes in different locations.

2. SYSTEM MODEL AND MAC DESIGN OBJECTIVE

In this section, we introduce the system model and the signal field reconstruction distortion measure, which leads to a simple MAC design objective.

2.1. Signal field model

Consider a one-dimensional field of unit length, denoted by $\mathcal{A} = [0, 1]$. Let $S(x)$ $(x \in \mathcal{A})$ be the source of interest in $\mathcal{A}$ at a particular time. We assume that the spatial dynamic of $S(x)$ is a homogeneous Gaussian random field given by the following linear stochastic differential equation:

$$dS(x) = -fS(x)dx + \sigma dW(x), \tag{1}$$

where $f > 0$, σ are known, $\{W(x) : x \geq 0\}$ is a standard Brownian motion, and $S(x) \sim \mathcal{N}(0, \sigma^2/|2f|)$ is the stationary solution of (1). The random field modeled in (1) is essentially a diffusion process which is often used to model many physical phenomena of interest. Being homogeneous in $\mathcal{A}$, $S(x)$ has the autocorrelation

$$E\{S(x_0)S(x_1)\} = \frac{\sigma^2}{2f}e^{-f(x_1-x_0)} \tag{2}$$

for $x_0 < x_1$, which is only a function of the distance between the two points x_1 and x_0.

2.2. Sensor network model

We assume that sensors in $\mathcal{A}$ are deployed randomly, and their distribution forms a one-dimensional homogeneous spatial Poisson field with local density ρ sensors/unit area. That is, in a length-l interval, the number of sensors $N(l)$ is a Poisson random variable with distribution

$$\mathcal{P}_r\{N(l) = k\} = e^{-\rho l}\frac{(\rho l)^k}{k!}, \tag{3}$$

and the numbers of sensors in any two disjoint intervals are independent. To avoid the boundary effect, we assume that there is a sensor at each of the two boundary points $x = 0$ and $x = 1$. Let N denote the number of sensors in the field excluding the two boundary points. Denote $\mathbf{x}_N = [x_1, x_2, \ldots, x_N]^T$ the sensor locations, where $0 < x_1 < x_2 < \cdots < x_N < 1$.

After its deployment, each sensor obtains its own location information through some positioning method. At a prearranged time, all sensors measure their local signals,

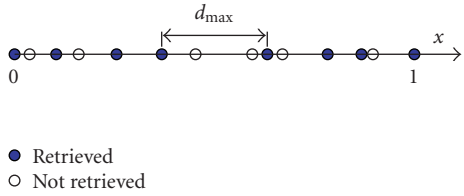

Figure 2: Linear field.

forming a snapshot of the signal field. The measurement of a sensor at location x is given by

$$Y(x) = S(x) + Z(x), \tag{4}$$

where $Z(x)$ is zero mean, spatially white Gaussian measurement noise with variance σ_Z^2, and is independent of $S(x)$.

Each sensor stores its local measurement along with its location information in the form of a packet for future data collection.

2.3. The multiple-access channel

When the mobile access point is ready for data collection, sensors transmit their measurement packets to the access point through a common wireless channel. We assume slotted transmission in a collision channel, that is, a packet is correctly received if and only if no other users attempt transmission. To retrieve measurement packets from the field through a collision channel, some form of MAC is needed. In this paper, we propose and discuss four MAC protocols, with different performance and complexity trade-off, to optimize the reconstruction performance.

In each time slot, sensors compete for the channel use. The channel output may be a collision, an empty slot, or a data packet that contains the measurement and the location of the sensor. We assume that the access point uses m time slots to retrieve measurement data and refer to m as the packet collection size. Let q_i, $1 \le i \le m$, denote the sample location of the ith channel outcome if a packet is successfully received. Otherwise, let $q_i = \varnothing$. Let $\mathbf{q} = [q_1, q_2, \ldots, q_m]^T$ denote the output location vector. To avoid the boundary effect for signal reconstruction, we assume that, in addition to the m retrieval attempts, the two boundary measurements are also retrieved by the mobile access point.

2.4. Information processing and performance measure

After the information retrieval, we reconstruct the original signal field based on the received data samples. Let K denote the number of q_i's not equal to $\varnothing$ in $\mathbf{q}$, excluding the two boundary points. Let $\mathbf{r}_K = [r_1, r_2, \ldots, r_K]^T$, $r_1 \le r_2 \le \cdots \le r_K$, be the ordered sample location vector constructed from $\mathbf{q}$ by ordering the non-$\varnothing$ elements. For convenience, let $r_0 = 0$ and $r_{K+1} = 1$.

We estimate $S(x)$ at location x using its two immediate neighbor samples by the MMSE smoothing, that is, for $r_i < x < r_{i+1}$, $0 \le i \le K$,

$$\hat{S}(x) = E\{S(x) | Y(r_i), Y(r_{i+1})\}. \tag{5}$$

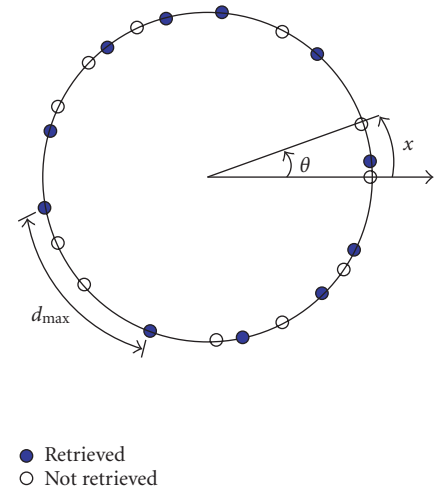

Figure 3: Circular field.

Given $\mathbf{q}$, we define *the maximum field reconstruction distortion* as he maximum mean-square estimation error in $\mathcal{A}$,

$$\mathcal{E}(\mathbf{q}) \triangleq \max_{x \in \mathcal{A}} E\{ |\hat{S}(x) - S(x)|^2 | \mathbf{q}\}. \tag{6}$$

The expected maximum distortion of the signal reconstruction in m collection time slots is then given by

$$\bar{\mathcal{E}}(m) \triangleq E\{\mathcal{E}(\mathbf{q})\}, \tag{7}$$

where the expectation is taken over the output location vector $\mathbf{q}$.

2.5. MAC design objective

Our objective is to design MAC protocols that result in the smallest signal field reconstruction distortion for a fixed number of retrieval slots. From [7, 8], we have shown that the maximum distortion is determined only by the maximum distance between two adjacent data samples,

$$\mathcal{E}(\mathbf{q}) = \frac{2f\sigma_Z^2/\sigma^2 + 1 - e^{-f d_{\max}(\mathbf{q})}}{2f\sigma_Z^2/\sigma^2 + 1 + e^{-f d_{\max}(\mathbf{q})}} \frac{\sigma^2}{2f} \triangleq \mathcal{E}(d_{\max}(\mathbf{q})), \tag{8}$$

where

$$d_{\max}(\mathbf{q}) = \max_{0 \le i \le K} (r_{i+1}(\mathbf{q}) - r_i(\mathbf{q})). \tag{9}$$

The maximum distortion in (6) is a monotonically increasing function of $d_{\max}$. Thus, a smaller $E\{d_{\max}\}$ indicates a smaller reconstruction distortion. Our objective now is to design MAC for the minimum $E\{d_{\max}\}$.

2.6. Linear field and circular field

The above 1D field model with two boundary points is referred to as *the linear field* (Figure 2). Another filed of interest is *the circular field* which is a circle with unit circumference (Figure 3). As in the linear field, sensors in the circular field are deployedaccording to Poisson distribution with density ρ

sensors/unit length; see (3). The location of each sensor on the circular field is described by its angle θ, $0 \le \theta < 2\pi$, as shown in Figure 3. Alternatively, the location can also be described by $x = \theta/2\pi$, $0 \le x < 1$. Let $\mathbf{x}_N = [x_1, x_2, \ldots, x_N]^T$, $x_1 \le x_2 \le \cdots \le x_N$, denote the sensor locations where N is the number of sensors in the field.[1]

Similar to the linear field, let $\mathbf{q} = [q_1, q_2, \ldots, q_m]^T$ denote the output location vector, where q_i, $1 \le i \le m$, is the sample location of the ith channel outcome if a packet is successfully received in the ith slot, or $q_i = \varnothing$ otherwise. Let K be the number of non-$\varnothing$ elements in $\mathbf{q}$ and let $\mathbf{r}_K = [r_1, r_2, \ldots, r_K]^T$ be the ordered sample location vector constructed from $\mathbf{q}$ by ordering the non-$\varnothing$ elements, with r_1 being the smallest. For convenience, let $r_{K+1} = 1 + r_1$. The maximum distance for the circular field is defined as

$$d_{\max}(\mathbf{q}) \triangleq \max_{1 \le i \le K} (r_{i+1}(\mathbf{q}) - r_i(\mathbf{q})). \tag{10}$$

To avoid ambiguity, define $d_{\max}$ to be 1 if only one sample is retrieved, or 2 if none is retrieved. Since we are not working in the extremely low-density regime, the probability of retrieving only one or no sample is small. Besides the vector form as in (9) and (10), the input parameters of $d_{\max}(\mathbf{q})$ for both fields also take other forms in this paper for the ease of presentation. The MAC design objective for the circular field is also to minimize $E\{d_{\max}\}$.

3. MAC FOR OPTIMAL INFORMATION RETRIEVAL PATTERN

3.1. Optimal centralized scheduling

Assume that the location information $\mathbf{x}_N$ of all sensors is available to the mobile access point. Also assume that the mobile access point is able to activate individual nodes for data transmission. The mobile access point is then able to precompute the optimal set of m locations and to activate only those sensors. This results in the minimum $d_{\max}$, and therefore, the best performance. The performance under this scheduler can be used as a benchmark for performance comparison.

For a given sensor location realization $\mathbf{x}_N$ and a fixed m, the optimal $d_{\max}$ is

$$d^*_{\max}(\mathbf{x}_N, m) = \min_{1 \le i_1 \le i_2 \le \cdots \le i_m \le N} d_{\max}(x_{i_1}, x_{i_2}, \ldots, x_{i_m}). \tag{11}$$

The optimal set of sensor locations are those that produce $d^*_{\max}$, and the mobile access point activates these sensors one at a time to avoid collision.

The optimization problem (11) can be solved by a brute force search. To reduce the computational complexity, we propose an efficient algorithm for the linear field, Algorithm 1. It first looks for an initial set of locations and the corresponding $d_{\max}$. Based on this $d_{\max}$, it looks for another set of locations resulting in a smaller $d_{\max}$. Iteratively, $d_{\max}$ converges to its minimum value in finite steps.

The search scheme consists of three steps.
Step 1. Location initialization. A set of m sensor locations is chosen from $\mathbf{x}_N$ as the initial set, $(q_1^{(0)}, \ldots, q_m^{(0)})$. The $d_{\max}$ of the chosen set is assigned to $d^{(0)}_{\max}$. Let $i = 0$.
Step 2. Within interval $(0, d^{(i)}_{\max})$, find the sensor location closest to $d^{(i)}_{\max}$ and assign it to $q_1^{(i+1)}$. For $1 \le j \le m-1$, if $q_j^{(i+1)} + d^{(i)}_{\max} > 1$, let $q_{j+1}^{(i+1)} = 1$; if $q_j^{(i+1)} + d^{(i)}_{\max} \le 1$ and there exists at least one sensor in the interval $(q_j^{(i+1)}, q_j^{(i+1)} + d^{(i)}_{\max})$, let $q_{j+1}^{(i+1)}$ be the sensor location closest to the right boundary of the interval; if $q_j^{(i+1)} + d^{(i)}_{\max} \le 1$ and there are no sensors in the interval $(q_j^{(i+1)}, q_j^{(i+1)} + d^{(i)}_{\max})$, the algorithm ends and $d^{(i)}_{\max}$ obtained previously is the minimum $d^*_{\max}$.
Step 3. After obtaining $q_1^{(i+1)}, \ldots, q_m^{(i+1)}$, calculate $d^{(i+1)}_{\max} = d_{\max}(q_1^{(i+1)}, \ldots, q_m^{(i+1)})$. If $d^{(i+1)}_{\max} < d^{(i)}_{\max}$, let $i = i + 1$ and go to Step 2. Otherwise, the search ends and $d^{(i)}_{\max}$ is the minimum $d^*_{\max}$.
When the search stops, the corresponding $(q_1^{(i)}, q_2^{(i)}, \ldots, q_m^{(i)})$ is the optimal set of locations for the given $\mathbf{x}_N$ and m. We select the initial set as follows. Choose $q_i^{(0)}$ to be the sensor location that is closest to $i/(m+1)$, $1 \le i \le m$, and let the corresponding $d_{\max}$ be $d^{(0)}_{\max}$.

Algorithm 1

Algorithm 1 stops only when $d^{(i)}_{\max}$ has reached its minimum value. For a field with finite sensors, the possible values of $d_{\max}$ is finite. Therefore, Algorithm 1 finds the optimal locations in finite steps.

Next, we consider the circular field. Algorithm 1 can be adapted to solve the optimization of (11) by converting the circular field to the linear field. For the ease of discussion, for a given $\mathbf{x}_N$, let $x_{N+j} \triangleq 1 + x_j$, $1 \le j \le N$. Suppose that x_i is included in the optimal set, $1 \le i \le N$. Then we break the circle at point x_i, and $(x_{i+1}, \ldots, x_{N+i-1})$ are sensor locations in the linear field with x_i and x_{N+i} being the two boundary points. The other $m-1$ points that minimize $d_{\max}$ under the assumption that x_i is selected can be solved by Algorithm 1.[2] Exhausting all x_i gives the global optimal $d^*_{\max}$. To shorten the search time, use the smallest $d_{\max}$ obtained in previous runs of Algorithm 1 as the initialization value $d^{(0)}_{\max}$ for the new search with a new x_i. It can be shown that exhausting $x_1 \le x_i < x_1 + d'_{\max}$ is enough, where $d'_{\max}$ is any value greater than or equal to the global minimum $d^*_{\max}$. The initialization value $d^{(0)}_{\max}$ for the current x_i can be used as $d'_{\max}$ for the exhaustion stopping criterion.

The centralized scheme gives the best performance under the condition that all sensor location information is available to the mobile access point. However, the bandwidth required for sensors reporting their locations is prohibitively

[1] We are reusing notations for the circular field. If a discussion is particular to the linear or the circular field, the notations should be understood in that context.

[2] Here, $m-1$ points are sought instead of m points in the linear field case.

large, especially for large-scale sensor networks. Decentralized schemes that do not require the knowledge of sensor locations at the mobile access point are desirable. Nonetheless, the centralized scheme gives the best possible performance and serves as a benchmark.

3.2. Decentralized scheduling through carrier sensing

In practice, the sensor location information may not be available at the mobile access point. Each senor only knows its own location. In this case, in order to retrieve data with the desired pattern and in a decentralized fashion, we propose decentralized scheduling through carrier sensing. We assume that each sensor has a transmission coverage radius R. Since the propagation delay is relatively small as compared to the slot length, we assume perfect carrier sensing with no propagation delay within radius R, that is, a sensor's transmission is detected immediately by other sensors within distance R.

In the proposed protocol, sensor transmissions are scheduled through carrier sensing, where the distances of sensors from the desired locations are used in the backoff scheme. The backoff time of a sensor is a function of the distance from the sensor to the desired location. A similar idea of using carrier sensing for decentralized transmission was first proposed in [9, 10, 11], where the channel state information was used in the backoff function of the carrier sensing scheme for opportunistic transmission.

Protocol. In each time slot, a segment of length R is activated. Sensors within the activated region compete for the channel use. Let p_j denote the center of the jth segment, $1 \le j \le m$. Each sensor within the activated segment computes its distance to p_j, that is, if x_i is within the activated segment, its distance is $d_{i,j} = |x_i - p_j|$ for the linear field, or $d_{i,j} = \min(|x_i - p_j|, 1 - |x_i - p_j|)$ for the circular field. The activated sensors then choose their respective backoff time based on a backoff function $\tau(d)$, which maps the distance to a backoff time. A sensor listens to the channel during its backoff time. If it detects a transmission before its backoff timer expires, the sensor will not transmit in this time slot. Otherwise, the sensor transmits its measurement sample packet immediately when its timer expires. The function $\tau(d)$ is designed to be strictly increasing; therefore, if there are sensors in the activated region, only the sensor closest to the center of the activated segment will be received successfully in this time slot. An example of $\tau(d)$ is given in Figure 4. The activation sequence is deterministic in the sense that it does not change based on the previous data collection results.

Where the activation segments should be centered is a design issue. As the next lemma shows, for the circular field, the segments should be separated evenly.

Lemma 1. *Consider the circular field. Suppose that in the* ith *time slot,* $1 \le i \le m$, *the length-*L *segment centered at* p_i, $0 \le p_i < 1$, *is activated to compete for the collision channel use. Suppose that these segments do not overlap. Let* q_i, $0 \le q_i < 1$, *be the outcome location in the* ith *slot if a packet is successfully received, or* $q_i = \varnothing$ *otherwise. Define the relative outcome location* b_i, $b_i = \varnothing$ *or* $-L/2 \le b_i \le L/2$, *as follows:*

$$b_i(p_i, q_i) \triangleq \begin{cases} \varnothing & \text{if } q_i = \varnothing, \\ q_i - p_i & \text{if } |q_i - p_i| \le \dfrac{L}{2}, \\ q_i - p_i - 1 & \text{if } |q_i - p_i| > \dfrac{L}{2},\ q_i > p_i, \\ q_i - p_i + 1 & \text{if } |q_i - p_i| > \dfrac{L}{2},\ q_i < p_i, \end{cases} \tag{12}$$

where the conditions in (12) *are to deal with the coordinate transition around* $\theta = 0$ *or* $\theta = 2\pi$ *on the circular field. If* b_i*'s are independent and identically distributed (i.i.d.), then evenly spaced segments produce the minimum* $E\{d_{\max}\}$ *for the circular field.*

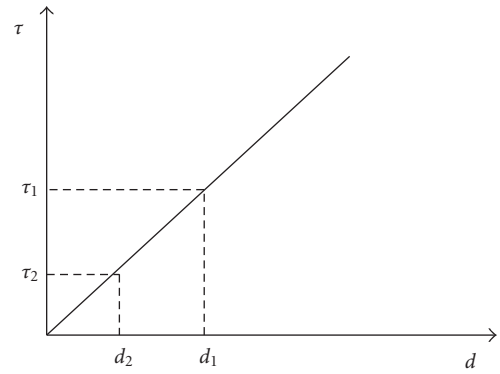

Figure 4: Backoff function $\tau(d)$.

For the proof, see Appendix A.

For the linear field, however, evenly spaced activation segment sequence is not optimal because of the asymmetry introduced by the two boundary points. Nonetheless, evenly spaced segment sequence has good performance for large m and ρ since the boundary effect is negligible in this scenario. We will use the evenly spaced segment sequence $p_i = i/(m+1)$, $1 \le i \le m$, for the linear field in the simulations.

The carrier sensing protocol has high throughput because, if there are nodes within an activation segment, the packet closest to the center will be successfully received with probability one.

3.3. Aloha scheduling

The carrier sensing scheme requires additional hardware for the carrier sensing functionality. In addition, the synchronization and timing requirements are strict for the carrier sensing mechanism. Next, we present a cost-efficient protocol for sensor sample collection.

Protocol. Select a sequence of m nonoverlapping length-ϵ segments as the activation sequence. Activate one segment in the activation sequence every time slot. Sensors within the activated region transmit their packet independently with probability P. The activation sequence is deterministic in the

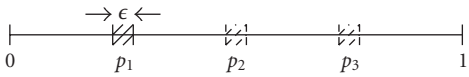

Figure 5: Aloha scheme on the linear field. A sequence of length-ϵ segments is activated sequentially. The sensors within the activated range transmit with probability P.

sense that it does not depend on the data collection results. Figure 5 illustrates the Aloha scheme on the linear field.

In the Aloha protocol, the segment length ϵ, the transmission probability P, and the center locations of the activation segments are optimization parameters.

Lemma 2. *For both the linear and the circular fields, the optimal transmission probability P is one and the optimal segment length ϵ is strictly less than $1/\rho$.*

For the proof, see Appendix B.

It can be shown that the result of Lemma 2 also holds in a more general setup where the transmission probability within the activation region is a function of the distance from the sensor to the center of the activation region. An intuitive way to explain Lemma 2 is that, for the same throughput, the smaller the activation interval length is, the more precise the outcome location can be. Therefore, the data collection outcomes for a smaller activation interval are closer to evenly spaced center locations, producing a smaller $E\{d_{\max}\}$. Letting $P = 1$ gives the smallest activation interval length for a given throughput. The result about ϵ can be explained as follows. Shortening the activation length has two effects on $E\{d_{\max}\}$: one is that it gives a lower throughput if the length is less than or equal to $1/\rho$, which is a negative effect; the other is that it produces a more precise outcome location control, a positive effect. Although ($P = 1$, $\epsilon = 1/\rho$) gives the maximum throughput for Aloha, when ϵ is shortened a little, the throughput only decreases a little because the derivative of the throughput with respect to ϵ is zero at $\epsilon = 1/\rho$. Thus the negative effect is small. The positive effect from the more precise location control favors an activation length strictly shorter than $1/\rho$, meaning that the optimal throughput is strictly less than $1/e$. Nonetheless, the gain by selecting a length shorter than $1/\rho$ is small for dense sensor networks. We will use $\epsilon = 1/\rho$ in the simulations.

As shown in Lemma 1, for the circular field, evenly spaced center locations of the activation segments are optimal. As mentioned in the carrier sensing protocol, for the linear field, evenly spaced activation segments are not optimal. Nonetheless, evenly spaced segments have good performance for large m and ρ, and we will use evenly spaced activation segments in the simulations for the linear field.

3.4. Adaptive Aloha scheduling

The carrier sensing and Aloha scheduling protocols presented previously are deterministic scheduling since the center location of each activation segment does not change according to previous data collection outcomes. In deterministic scheduling, the activation location information may be preset to sensors before their deployment, eliminating the need to broadcast the location information from the mobile access point and saving some hardware cost. Another approach is to let the mobile access point decide the next activation location on the fly, based on previous data collection results. Allowing the activation sequence to adapt to previous data collection results may give better performance. Next we present an adaptive scheduling for Aloha.

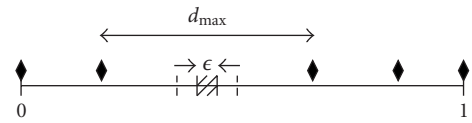

Figure 6: Adaptive Aloha scheduling example on the linear field. The mobile access point activates one interval of length ϵ in one time slot. The sensors within the activated range transmit with probability $P = 1$. The solid diamonds indicate the received packets. The algorithm tries to break the maximum distance by placing the next polling interval at the center of the two received data sample locations whose distance is $d_{\max}$.

Protocol. The basic activation strategy is similar to the Aloha protocol. The mobile access point activates an interval of length $\epsilon = 1/\rho$ in each time slot; the sensors within the range transmit with probability $P = 1$. The difference is that, in the adaptive version, the locations of the activation intervals depend on the previous data collection results, which is described as follows.

After obtaining a new packet, the access point checks all the previous received data and finds the two adjacent sample locations that have the maximum distance. The access point then locates the next polling interval in the middle of these two samples locations (see Figure 6 for the linear field case). If an empty slot occurs, the access point then activates the length-ϵ interval adjacent (either left or right) to the previous empty intervals until a success or collision occurs. If a collision occurs, the access point resolves the collision by splitting the collision interval until a packet is successfully received (similar to the splitting algorithms [12]). If a packet is received successfully, the access point recalculates and tries to break the new $d_{\max}$ of the received samples within the remaining time slots. The algorithm keeps running until it uses up the m time slots.

The above protocol works in an environment where the mobile access point can communicate to the whole field from one location, for example, high-altitude airplanes or satellites. There are other types of adaptive scheduling schemes. For example, we can also adapt the activation sequence on a carrier sensing scheduling setup. However, as will be shown in the simulations section, the gain of adapting activation sequence on a carrier sensing setup is small because the performance of the carrier sensing scheduling is already close to that of the optimal centralized scheduling.

4. SIMULATIONS

In this section, we compare the performance of the MAC protocols proposed in the last section through simulations. Due to the space limit, only figures for the linear field are

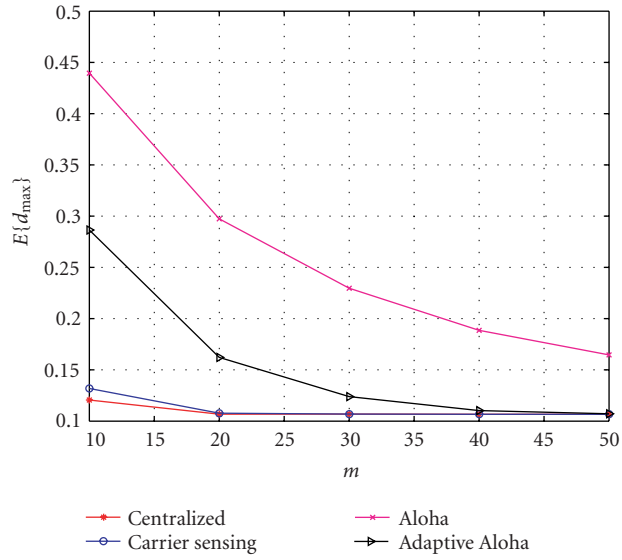

FIGURE 7: $E\{d_{\max}\}$ versus packet collection size m for sensor density $\rho = 40$.

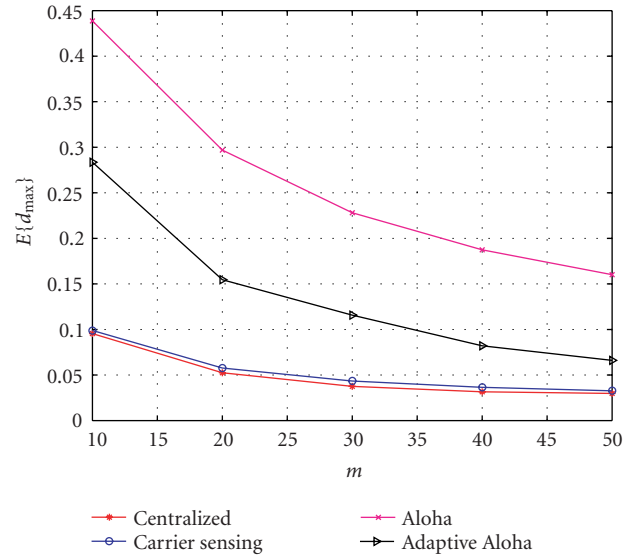

FIGURE 8: $E\{d_{\max}\}$ versus packet collection size m for sensor density $\rho = 200$.

shown. For the circular field, similar results are observed. Sensors are randomly deployed according to the Poisson distribution with density ρ. For convenience, we name these MAC protocols as follows.

(i) π_1 is the optimal centralized scheduler.
(ii) π_2 is the decentralized scheduling through carrier sensing with $R = 1$.
(iii) π_3 is the Aloha scheduling.
(iv) π_4 is the adaptive Aloha scheduling.

We use the $d_{\max}$ found using π_2 as the initial maximum distance for the iteration algorithm in π_1. The search stops after 1-2 iterations typically. In the comparison, we use $E\{d_{\max}\}$ as the performance metric.

Figures 7 and 8 plot $E\{d_{\max}\}$ versus m for sensor density $\rho = 40$ and 200, respectively. The expectation of $d_{\max}$ in the figures is averaged over 100 000 realizations of the Poisson sensor field. As expected, as m increases, the number of data samples received at the mobile access point increases, and thus $E\{d_{\max}\}$ decreases. We see that there is little performance loss by using π_2. Notice that, when m is larger than ρ (Figure 7), under π_1 and π_2, data from all sensors can be retrieved with a high probability. Therefore, the performance gap for the two protocols diminishes. The performance under π_3 is worse than other schemes even when m is larger than ρ. This is because, under π_3, some scheduled intervals do not have data packets received successfully due to either collision or void of sensors. Unlike π_3, the location of each activation interval of π_4 is adapted to the previous data collection outcomes. When m is large, it has enough slots to search for intervals within which sensors exist and to resolve collision, therefore avoiding the problem in π_3. From Figure 7, we see that, when m is large, the performance under π_4 is as good as the optimal case.

Figures 9 and 10 plot $E\{d_{\max}\}$ versus ρ for packet collection size $m = 10$ and 50, respectively. As expected, as ρ increases, the density of the sensor field increases, and the received data locations are closer to the desired locations, resulting in a sample pattern closer to evenly spaced. Therefore, $E\{d_{\max}\}$ converges to the minimum value as ρ increases. Again, we see that the performance under π_2 closely follows the optimal one. As ρ increases, we see the performance gap between the two Aloha schemes and π_1 increases. The performance loss under π_3 is mainly due to its lower throughput than that of π_1 and π_2, which limits the number of received samples. We observe that there is a significant performance improvement of π_4 over π_3 by adaptively optimizing the retrieval pattern based on the retrieval history.

5. CONCLUSION

To reconstruct the signal field using sensor networks, the locations of the retrieved data affect the signal field reconstruction performance. In this paper, we design MAC protocols to obtain the desired data retrieval pattern. We propose a new MAC design criterion that takes into account the application characteristics of the signal field reconstruction. Taking both performance and implementation complexity into consideration, besides the optimal centralized scheduler, we propose three decentralized MAC protocols. We have shown that, for the carrier sensing and Aloha scheduling schemes, evenly spaced activation intervals are optimal for the circular field. For the Aloha scheduling in both the linear field and the circular field, the optimal transmission probability is one and the optimal activation interval length is strictly smaller than $1/\rho$, resulting in a throughput strictly less than $1/e$. Our simulations show that using the decentralized scheduling through carrier sensing results in little performance loss

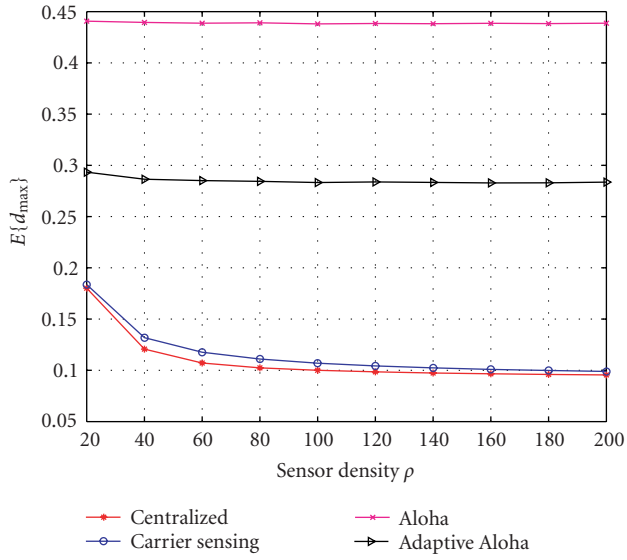

FIGURE 9: $E\{d_{\max}\}$ versus sensor density ρ for packet collection size $m = 10$.

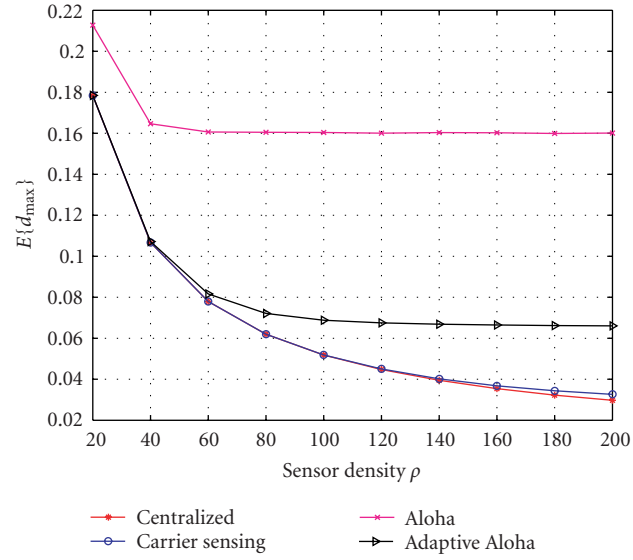

FIGURE 10: $E\{d_{\max}\}$ versus sensor density ρ for packet collection size $m = 50$.

compared to the performance of the optimal scheduler. For the two Aloha schemes, by exploring the history of retrieved data locations, adaptive Aloha provides a significant performance gain over the simple Aloha scheme.

APPENDICES

A. PROOF OF LEMMA 1

We first define four operations on integers or real numbers. Let i and j be two integers. Define $i \oplus j$ to be equal to $i+j+km$, where k is the integer such that $1 \le i + j + km \le m$. Let $i \ominus j \triangleq i \oplus (-j)$. Let x_1 and x_2 be two real numbers. Define $x_1 \oplus x_2$ to be equal to x_1+x_2+k, where k is the integer such that $0 \le x_1+x_2+k < 1$. Let $x_1 \ominus x_2 \triangleq x_1 \oplus (-x_2)$. For convenience, extend the operations $\bigoplus$ and $\bigominus$ on real numbers to include the symbol $\varnothing$. Let x_1 and x_2 be real numbers or the symbol $\varnothing$. Define $x_1 \oplus x_2$ and $x_1 \ominus x_2$ to be $\varnothing$ if either x_1 or x_2 is equal to $\varnothing$.

It can be verified that the inverse function of (12) is given by

$$q_i(p_i, b_i) = p_i \oplus b_i. \tag{A.1}$$

The average $d_{\max}$ when $\mathbf{p}$ is the center location vector is given by

$$E_{\mathbf{q}}\{d_{\max}(\mathbf{q}); \mathbf{p}\} = E_{\mathbf{b}}\{d_{\max}(\mathbf{p} \oplus \mathbf{b})\}, \tag{A.2}$$

where $\mathbf{p} \oplus \mathbf{b}$ is the vector with $p_i \oplus b_i$ as the ith entry. Without loss of generality, assume that $\mathbf{p}$ is an ordered vector with p_1 being the smallest. Let $\tilde{\mathbf{p}}$ be an equally spaced location vector on the circular field. Without loss of generality, let $\tilde{p}_i = (i-1)/m$, $1 \le i \le m$. The proof is concluded if we show that, for all $\mathbf{p}$,

$$E_{\mathbf{b}}\{d_{\max}(\mathbf{p} \oplus \mathbf{b})\} \ge E_{\mathbf{b}}\{d_{\max}(\tilde{\mathbf{p}} \oplus \mathbf{b})\}. \tag{A.3}$$

Let $\mathbf{b}^{(k)}$ be the kth rotated vector of $\mathbf{b}$, that is, $b_i^{(k)} = b_{i \oplus k}$, for $0 \le k \le m-1$ and $1 \le i \le m$. Since b_i's are i.i.d., we have, for $0 \le k \le m-1$,

$$E_{\mathbf{b}}\{d_{\max}(\mathbf{p} \oplus \mathbf{b})\} = E_{\mathbf{b}}\{d_{\max}(\mathbf{p} \oplus \mathbf{b}^{(k)})\}. \tag{A.4}$$

Therefore, the left-hand side of (A.3) can be expressed as

$$E_{\mathbf{b}}\left\{\frac{1}{m}\sum_{k=0}^{m-1} d_{\max}(\mathbf{p} \oplus \mathbf{b}^{(k)})\right\}. \tag{A.5}$$

Hence, it suffices to show that for any $\mathbf{b}$ and $\mathbf{p}$,

$$\frac{1}{m}\sum_{k=0}^{m-1} d_{\max}(\mathbf{p} \oplus \mathbf{b}^{(k)}) \ge d_{\max}(\tilde{\mathbf{p}} \oplus \mathbf{b}). \tag{A.6}$$

For a given $\mathbf{b}$ with one or no non-$\varnothing$ element, by definition, $d_{\max}$ is equal to 1 or 2, respectively, for both $\mathbf{p}$ and $\tilde{\mathbf{p}}$. Therefore, (A.6) holds.

Let $\mathcal{L}(i, j)$ be the set of indices between i and j counterclockwise, $1 \le i, j \le m$ and $i \ne j$, that is, $\mathcal{L}(i, j) = \{l : i < l < j\}$ if $i < j$, or $\{l : i < l \le m$, or $1 \le l < j\}$ if $i > j$. For a given $\mathbf{b}$ with at least two non-$\varnothing$ entries, search $d_{\max}$ among the output locations $\tilde{\mathbf{p}} \oplus \mathbf{b}$ on the circular field. Suppose that

$d_{\max}$ occurs from the ith point to the jth point counterclockwise, that is, $b_i, b_j \neq \emptyset$, $b_l = \emptyset$ for $l \in \mathcal{L}(i,j)$, and

$$\begin{aligned} d_{\max}(\tilde{\mathbf{p}} \oplus \mathbf{b}) &= (\tilde{p}_j \oplus b_j) \ominus (\tilde{p}_i \oplus b_i) \\ &= (\tilde{p}_j \ominus \tilde{p}_i) + (b_j - b_i) \qquad \text{(A.7)} \\ &= \left(\frac{j \ominus i}{m}\right) + (b_j - b_i), \end{aligned}$$

where (A.7) holds because $\tilde{p}_j \ominus \tilde{p}_i > L > b_j - b_i$. Since $b_l = \emptyset$ for $l \in \mathcal{L}(i,j)$, in the outcome locations $\mathbf{p} \oplus \mathbf{b}^{(k)}$, there are no valid samples from $p_{i\ominus k} \oplus b^{(k)}_{i\ominus k}$ counterclockwise to $p_{j\ominus k} \oplus b^{(k)}_{j\ominus k}$. Hence $d_{\max}(\mathbf{p} \oplus \mathbf{b}^{(k)})$ is at least as large as the distance from $p_{i\ominus k} \oplus b^{(k)}_{i\ominus k}$ counterclockwise to $p_{j\ominus k} \oplus b^{(k)}_{j\ominus k}$. Thus,

$$\begin{aligned} &\sum_{k=0}^{m-1} d_{\max}(\mathbf{p} \oplus \mathbf{b}^{(k)}) \\ &\quad \geq \sum_{k=0}^{m-1} \left(\left(p_{j\ominus k} \oplus b^{(k)}_{j\ominus k}\right) \ominus \left(p_{i\ominus k} \oplus b^{(k)}_{i\ominus k}\right)\right) \\ &\quad = \sum_{k=0}^{m-1} \left((p_{j\ominus k} \ominus p_{i\ominus k}) + (b_j - b_i)\right) \qquad \text{(A.8)} \\ &\quad = \left(\sum_{k=0}^{m-1} \sum_{l=1}^{j\ominus i} \left(p_{i\ominus k\oplus l} \ominus p_{i\ominus k\oplus l\ominus 1}\right)\right) + m(b_j - b_i) \\ &\quad = \left(\sum_{l=1}^{j\ominus i} \sum_{k=0}^{m-1} \left(p_{i\ominus k\oplus l} \ominus p_{i\ominus k\oplus l\ominus 1}\right)\right) + m(b_j - b_i) \\ &\quad = \sum_{l=1}^{j\ominus i} 1 + m(b_j - b_i) \qquad \text{(A.9)} \\ &\quad = (j \ominus i) + m(b_j - b_i) \\ &\quad = m\, d_{\max}(\tilde{\mathbf{p}} \oplus \mathbf{b}), \end{aligned}$$

where (A.8) holds because $p_{j\ominus k} \ominus p_{i\ominus k} > L > b_j - b_i$, and (A.9) holds because $\sum_{k=0}^{m-1}(p_{i\ominus k\oplus l} \ominus p_{i\ominus k\oplus l\ominus 1})$ is equal to the circumference of the circular field, which is one.

B. PROOF OF LEMMA 2

We prove Lemma 2 for the linear field. The proof for the circular field is basically the same except that extra care should be taken for coordinate transitions around location $x = 0$ or $x = 1$. Consider a more general scheme which does not require that each activation segment has the same length and transmission probability. Let p_i, P_i, and ϵ_i denote the center, the transmission probability, and the length of the ith activation segment, respectively, $1 \leq i \leq m$. Let q_i be the outcome location of the ith channel competition, or $q_i = \emptyset$ if no sample packet is received successfully in the ith time slot, due to either collision or no transmission. The throughput of the ith time slot is

$$s_i \triangleq \mathcal{P}_r\{q_i \neq \emptyset\} = \epsilon_i P_i \rho e^{-\epsilon_i P_i \rho}. \qquad \text{(B.10)}$$

Given a packet is received successfully in the ith time slot, the location q_i is uniformly distributed,

$$p(q_i | q_i \neq \emptyset) = \frac{1}{\epsilon_i} 1_{p_i - \epsilon_i/2 \leq q_i \leq p_i + \epsilon_i/2}, \qquad \text{(B.11)}$$

where 1_A is the indicator function. Let $\mathbf{q} = [q_1, \ldots, q_m]^T$. Since the activation segments do not overlap, q_i's are independent. Let $\mathbf{q}_{/i}$ denote the length-$(m-1)$ vector constructed by taking out q_i from $\mathbf{q}$. The expected $d_{\max}(\mathbf{q})$ is given by

$$\begin{aligned} &E_{\mathbf{q}}\{d_{\max}(\mathbf{q})\} \\ &= E_{\mathbf{q}_{/i}} E_{q_i}\{d_{\max}(\mathbf{q}_{/i}, q_i) | \mathbf{q}_{/i}\} \\ &= \frac{1}{2} E_{\mathbf{q}_{/i}} \Big\{ 2(1 - s_i) d_{\max}(\mathbf{q}_{/i}, q_i = \emptyset) \\ &\qquad + \frac{s_i}{\epsilon_i} \int_{-\epsilon_i/2}^{\epsilon_i/2} \Big(d_{\max}(\mathbf{q}_{/i}, q_i = p_i + a) \\ &\qquad\qquad + d_{\max}(\mathbf{q}_{/i}, q_i = p_i - a) \Big) \mathrm{d}a \Big\}. \end{aligned} \qquad \text{(B.12)}$$

Suppose that $(\tilde{\epsilon}_i, \tilde{P}_i)$ give the same throughput as (ϵ_i, P_i), that is, $\tilde{\epsilon}_i \tilde{P}_i \rho e^{-\tilde{\epsilon}_i \tilde{P}_i \rho} = s_i$. And suppose that $\tilde{\epsilon}_i < \epsilon_i$. We will show that if (ϵ_i, P_i) are replaced by $(\tilde{\epsilon}_i, \tilde{P}_i)$ while other parameters remain the same, then $E\{d_{\max}(\mathbf{q})\}$ decreases. Since the throughput s_i remains the same, the first term of (B.12) remains the same. If we can show that, for all $\mathbf{q}_{/i}$ and for $-\epsilon_i/2 \leq a \leq \epsilon_i/2$,

$$\begin{aligned} &d_{\max}(\mathbf{q}_{/i}, q_i = p_i + a) + d_{\max}(\mathbf{q}_{/i}, q_i = p_i - a) \\ &\qquad \geq d_{\max}\left(\mathbf{q}_{/i}, q_i = p_i + \frac{\tilde{\epsilon}_i}{\epsilon_i} a\right) + d_{\max}\left(\mathbf{q}_{/i}, q_i = p_i - \frac{\tilde{\epsilon}_i}{\epsilon_i} a\right), \end{aligned} \qquad \text{(B.13)}$$

then we have shown that the second term of (B.12) decreases. Therefore, we have proved that, with the same throughput, the shorter the activation length, the better the performance. Hence, the optimal P_i is 1 and the optimal ϵ_i is less than or equal to $1/\rho$ for all i because these conditions in Aloha give the shortest activation length for a given throughput.

Next we prove (B.13). Let length-m vectors $\mathbf{q}'$, $\tilde{\mathbf{q}}$, and $\tilde{\mathbf{q}}'$ be functions of $\mathbf{q}$ given $q_i \neq \emptyset$: $q'_j = \tilde{q}_j = \tilde{q}'_j = q_j$ for $j \neq i$, $q'_i = 2p_i - q_i$, $\tilde{q}_i = p_i + \tilde{\epsilon}_i/\epsilon_i(q_i - p_i)$, and $\tilde{q}'_i = p_i - \tilde{\epsilon}_i/\epsilon_i(q_i - p_i)$ (Figure 11). Equivalently, we are proving that

$$d_{\max}(\mathbf{q}) + d_{\max}(\mathbf{q}') \geq d_{\max}(\tilde{\mathbf{q}}) + d_{\max}(\tilde{\mathbf{q}}') \qquad \text{(B.14)}$$

for all $\mathbf{q}$ with $q_i \neq \emptyset$, or equivalently, for all $\tilde{\mathbf{q}}$ with $\tilde{q}_i \neq \emptyset$. We first define three terms for the ease of discussion. $d_{\max}(\mathbf{q})$ is said to be *associated* with q_i if q_i is one of the endpoints that produces $d_{\max}$ given $\mathbf{q}$ as the outcome location vector. $d_{\max}(\mathbf{q})$ is said to be associated with q_i *to the inside* if $d_{\max}(\mathbf{q})$ is associated with q_i and the center p_i is between the two endpoints of $d_{\max}$. $d_{\max}(\mathbf{q})$ is said to be associated with q_i *to the outside* if $d_{\max}(\mathbf{q})$ is associated with q_i and the center p_i is

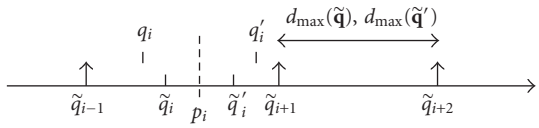

Figure 11: Case 1.

not between the two endpoints of $d_{\max}$. We prove (B.14) by verifying all possible cases.

Case 1. Neither $d_{\max}(\tilde{\mathbf{q}})$ is associated with $\tilde{q}_i$ nor $d_{\max}(\tilde{\mathbf{q}}')$ is associated with $\tilde{q}_i'$. Therefore, $d_{\max}(\tilde{\mathbf{q}})$ and $d_{\max}(\tilde{\mathbf{q}}')$ are associated with two points other than $\tilde{q}_i$ or $\tilde{q}_i'$ (Figure 11). Since these two points are also adjacent points in $\mathbf{q}$ and $\mathbf{q}'$, $d_{\max}(\mathbf{q})$ and $d_{\max}(\mathbf{q}')$ are at least as large as the distance of the two points. Therefore, $d_{\max}(\mathbf{q}) + d_{\max}(\mathbf{q}') \geq d_{\max}(\tilde{\mathbf{q}}) + d_{\max}(\tilde{\mathbf{q}}')$.

Case 2. Either $d_{\max}(\tilde{\mathbf{q}})$ is associated with $\tilde{q}_i$ to the outside or $d_{\max}(\tilde{\mathbf{q}}')$ is associated with $\tilde{q}_i'$ to the outside. Without loss of generality, assume that $d_{\max}(\tilde{\mathbf{q}}')$ is associated with $\tilde{q}_i'$ to the outside (Figure 12). Suppose that the other endpoint for $d_{\max}(\tilde{\mathbf{q}}')$ is $\tilde{q}_k$, $k \neq i$. By assumption, $\tilde{q}_k$ and $\tilde{q}_i'$ are on the same side of p_i. Thus, it can be verified that $\tilde{q}_i$ and $\tilde{q}_k$ are the two endpoints of $d_{\max}(\tilde{\mathbf{q}})$. Therefore,

$$d_{\max}(\tilde{\mathbf{q}}) + d_{\max}(\tilde{\mathbf{q}}') = 2\,|\,p_i - \tilde{q}_k\,|. \tag{B.15}$$

Since q_i and $\tilde{q}_k$ are two adjacent points in $\mathbf{q}$, we have $d_{\max}(\mathbf{q}) \geq |q_i - \tilde{q}_k|$. Similarly, $d_{\max}(\mathbf{q}') \geq |q_i' - \tilde{q}_k|$. Since q_i and q_i' are on the same side of $\tilde{q}_k$, we have

$$\begin{aligned} d_{\max}(\mathbf{q}) + d_{\max}(\mathbf{q}') &\geq |\,q_i - \tilde{q}_k\,| + |\,q_i' - \tilde{q}_k\,| \\ &= 2\,|\,p_i - \tilde{q}_k\,| \\ &= d_{\max}(\tilde{\mathbf{q}}) + d_{\max}(\tilde{\mathbf{q}}'). \end{aligned} \tag{B.16}$$

Case 3. Either $d_{\max}(\tilde{\mathbf{q}})$ is associated with $\tilde{q}_i$ to the inside or $d_{\max}(\tilde{\mathbf{q}}')$ is associated with $\tilde{q}_i'$ to the inside, but neither $d_{\max}(\tilde{\mathbf{q}})$ is associated with $\tilde{q}_i$ to the outside nor $d_{\max}(\tilde{\mathbf{q}}')$ is associated with $\tilde{q}_i'$ to the outside. Without loss of generality, assume that $d_{\max}(\tilde{\mathbf{q}})$ is associated with $\tilde{q}_i$ to the inside (Figure 13). Since q_i is further away from the center p_i than $\tilde{q}_i$, we have $d_{\max}(\mathbf{q}) > d_{\max}(\tilde{\mathbf{q}})$. There are two subcases.

Subcase 1. $d_{\max}(\tilde{\mathbf{q}}')$ is associated with $\tilde{q}_i'$ to the inside. Since q_i' is further away from the center p_i than $\tilde{q}_i'$, we have $d_{\max}(\mathbf{q}') > d_{\max}(\tilde{\mathbf{q}}')$. Therefore,

$$d_{\max}(\mathbf{q}) + d_{\max}(\mathbf{q}') > d_{\max}(\tilde{\mathbf{q}}) + d_{\max}(\tilde{\mathbf{q}}'). \tag{B.17}$$

Subcase 2. $d_{\max}(\tilde{\mathbf{q}}')$ is not associated with $\tilde{q}_i'$. With the same argument as in Case 1, we have $d_{\max}(\mathbf{q}') \geq d_{\max}(\tilde{\mathbf{q}}')$. Therefore, (B.17) still holds.

The above three cases conclude the proof of (B.14). Thus we have shown that the optimal P_i is 1 and the optimal ϵ_i is less than or equal to $1/\rho$ for all i. Next we prove that the optimal ϵ_i is strictly less than $1/\rho$. Since $E\{d_{\max}(\mathbf{q})\}$ is a continuous function of ϵ_i, it suffices to prove that, when $P = 1$,

$$\left.\frac{\partial E\{d_{\max}(\mathbf{q})\}}{\partial \epsilon_i}\right|_{\epsilon_i = 1/\rho} > 0. \tag{B.18}$$

From (B.12),

$$\begin{aligned} &\frac{\partial E\{d_{\max}(\mathbf{q})\}}{\partial \epsilon_i} \\ &\quad = \rho e^{-\epsilon_i \rho} E_{\mathbf{q}_{/i}} \left\{ (\epsilon_i \rho - 1) d_{\max}(\mathbf{q}_{/i},\ q_i = \varnothing) - \frac{\rho}{2} \int_{-\epsilon_i/2}^{\epsilon_i/2} \left(d_{\max}(\mathbf{q}_{/i},\ q_i = p_i + a) + d_{\max}(\mathbf{q}_{/i},\ q_i = p_i - a) \right) \mathrm{d}a \right. \\ &\qquad \left. + \frac{1}{2} \left(d_{\max}\left(\mathbf{q}_{/i},\ q_i = p_i + \frac{\epsilon_i}{2}\right) + d_{\max}\left(\mathbf{q}_{/i},\ q_i = p_i - \frac{\epsilon_i}{2}\right) \right) \right\}. \end{aligned} \tag{B.19}$$

The first term of (B.19) is equal to zero given that $\epsilon_i = 1/\rho$. From (B.13),

$$\begin{aligned} &d_{\max}\left(\mathbf{q}_{/i},\ q_i = p_i + \frac{\epsilon_i}{2}\right) + d_{\max}\left(\mathbf{q}_{/i},\ q_i = p_i - \frac{\epsilon_i}{2}\right) \\ &\geq d_{\max}(\mathbf{q}_{/i},\ q_i = p_i + a) + d_{\max}(\mathbf{q}_{/i},\ q_i = p_i - a) \end{aligned} \tag{B.20}$$

for $-\epsilon_i/2 < a < \epsilon_i/2$. Since (B.17) in Case 3 in the proof of the first part occurs with nonzero probability, strict inequality in (B.20) occurs with nonzero probability. Therefore, the sum of the second and the third terms of (B.19) is strictly larger than zero given that $\epsilon_i = 1/\rho$, thus proving (B.18).

ACKNOWLEDGMENTS

This work was supported in part by the National Science Foundation under Contract CCR-0311055, the

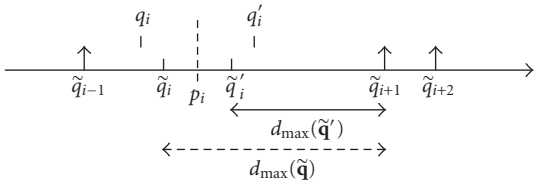

FIGURE 12: Case 2.

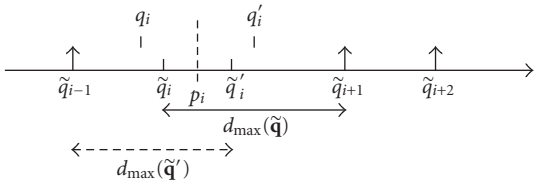

FIGURE 13: Case 3.

Multidisciplinary University Research Initiative (MURI) under the Office of Naval Research Contract N00014-00-1-0564, and the Army Research Laboratory CTA on Communication and Networks under Grant DAAD19-01-2-0011. Part of this work was presented at MILCOM, Monterey, Calif, USA, October 2004.

REFERENCES

[1] L. Tong, Q. Zhao, and S. Adireddy, "Sensor networks with mobile agents," in *Proc. IEEE Military Communications Conference (MILCOM '03)*, vol. 1, pp. 688–693, Boston, Mass, USA, October 2003.

[2] P. Venkitasubramaniam, S. Adireddy, and L. Tong, "Sensor networks with mobile access: optimal random access and coding," *IEEE J. Select. Areas Commun.*, vol. 22, no. 6, pp. 1058–1068, 2004.

[3] A. Woo and D. Culler, "A transmission control scheme for media access in sensor networks," in *Proc. 7th Annual ACM/IEEE International Conference on Mobile Computing and Networking (MobiCom '01)*, pp. 221–235, Rome, Italy, July 2001.

[4] W. Ye, J. Heidemann, and D. Estrin, "An energy-efficient MAC protocol for wireless sensor networks," in *Proc. 21st Annual Joint Conference of the IEEE Computer and Communications Societies (INFOCOM '02)*, vol. 3, pp. 1567–1576, New York, NY, USA, June 2002.

[5] K. Sohrabi, J. Gao, V. Ailawadhi, and G. J. Pottie, "Protocols for self-organization of a wireless sensor network," *IEEE Pers. Commun.*, vol. 7, no. 5, pp. 16–27, 2000.

[6] R. Iyer and L. Kleinrock, "QoS control for sensor networks," in *Proc. IEEE International Conference on Communications (ICC '03)*, vol. 1, pp. 517–521, Anchorage, Alaska, USA, May 2003.

[7] M. Dong, L. Tong, and B. M. Sadler, "Impact of MAC design on signal field reconstruction in dense sensor networks," submitted to *IEEE Trans. Signal Processing*.

[8] M. Dong, L. Tong, and B. M. Sadler, "Information retrieval and processing in sensor networks: deterministic scheduling vs. random access," in *Proc. IEEE International Symposium on Information Theory (ISIT '04)*, pp. 79–79, Chicago, Ill, USA, June–July 2004.

[9] Q. Zhao and L. Tong, "QoS specific medium access control for wireless sensor network with fading," in *Proc. 8th International Workshop on Signal Processing for Space Communications (SPSC '03)*, Catania, Italy, September 2003.

[10] Q. Zhao and L. Tong, "Distributed opportunistic transmission for wireless sensor networks," in *Proc. IEEE International Conference on Acoustics, Speech, and Signal Processing (ICASSP '04)*, vol. 3, pp. 833–836, Montreal, Quebec, Canada, May 2004.

[11] Q. Zhao and L. Tong, "Opportunistic carrier sensing for energy-efficient information retrieval in sensor networks," *EURASIP Journal on Wireless Communications and Networking*, vol. 2005, no. 2, pp. 231–241, 2005.

[12] D. Bertsekas and R. Gallager, *Data Networks*, Prentice-Hall, Englewood Cliffs, NJ, USA, 1992.

Zhiyu Yang received the B.Eng. degree in electronic engineering from Tsinghua University, Beijing, China, in 2000, and the S.M. degree in engineering sciences from Harvard University, Cambridge, Massachusetts, in 2001. Currently, he is a Ph.D. candidate in the School of Electrical and Computer Engineering, Cornell University, Ithaca, New York. His areas of interest include wireless communications, communication and sensor networks, information theory, and signal processing.

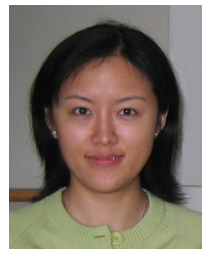

Min Dong received the B.Eng. degree from Tsinghua University, Beijing, China, in 1998, and the Ph.D. degree in electrical and computer engineering from Cornell University, Ithaca, New York, in 2004. She is currently with the Cooperate Research and Development, QUALCOMM Incorporated, San Diego, Calif, USA. Dr. Dong received the IEEE Signal Processing Society Best Paper Award in 2004. Her research interests include statistical signal processing, wireless communications, and communication networks.

Lang Tong is a Professor in the School of Electrical and Computer Engineering, Cornell University, Ithaca, New York. He received the B.E. degree from Tsinghua University, Beijing, China, in 1985, and M.S. and Ph.D. degrees in electrical engineering in 1987 and 1991, respectively, from the University of Notre Dame, Notre Dame, Indiana. He was a Postdoctoral Research Affiliate at the Information Systems Laboratory, Stanford University, in 1991. He was also the 2001 Cor Wit Visiting Professor at the Delft University of Technology. Dr. Tong received *Young Investigator Award* from the Office of Naval Research in 1996, the *Outstanding Young Author Award* from the IEEE Circuits and Systems Society in 1991, the 2004 IEEE Signal Processing Society Best Paper Award (with M. Dong), the 2004 Leonard G. Abraham Prize Paper Award from the IEEE Communications Society (with P. Venkitasubramaniam and S. Adireddy). He serves as an Associate Editor for the IEEE Transactions on Signal Processing and IEEE Signal Processing Letters. His areas of interest include statistical signal processing, wireless communications, communication networks and sensor networks, and information theory.

Brian M. Sadler received the B.S. and M.S. degrees from the University of Maryland, College Park, and the Ph.D. degree from the University of Virginia, Charlottesville, all in electrical engineering. He is a Senior Research Scientist at the Army Research Laboratory (ARL) in Adelphi, MD, USA. He was a Lecturer at the University of Maryland, and has been lecturing at Johns Hopkins University since 1994 on statistical signal processing and communications. He is an Associate Editor for the IEEE Signal Processing Letters, was an Associate Editor for the IEEE Transactions on Signal Processing, is on the editorial board for the EURASIP Journal on Wireless Communications and Networking, and is a Guest Editor for the IEEE JSAC special issue on Military Communications. He is a Member of the IEEE Technical Committee on Signal Processing for Communications, an IEEE Senior Member, and cochaired the 2nd IEEE Workshop on Signal Processing Advances in Wireless Communications (SPAWC-99). His research interests include signal processing for mobile wireless and ultra-wideband systems, and sensor signal processing and networking.